EUROPEAN ORGANIZATION FOR NUCLEAR RESEARCH

CERN-EP/88-64
14.6.1988

Nuclear Charge Radii of $^{78-100}$Sr by Non-Optical Detection in Fast-Beam Laser Spectroscopy

R.E. Silverans, P. Lievens and L. Vermeeren
Instituut voor Kern- en Stralingsfysika
Leuven University, B-3030 Leuven, Belgium

E. Arnold, W. Neu, R. Neugart and K. Wendt
Institut für Physik
Universität Mainz, D-6500 Mainz, Fed. Rep. Germany

F. Buchinger and E.B. Ramsay
Foster Radiation Laboratory
Mc Gill University, H3A2B2 Montreal, Canada

and

G. Ulm
The ISOLDE Collaboration
CERN, CH-1211 Geneva, Switzerland

(IS83)

We report the application of a new non-optical detection scheme in laser spectroscopy on ion beams of on-line isotope separators. The method consists of ground-state depopulation by optical pumping in collinear laser–ion-beam interaction, state selective neutralization, and charge-state separated fast-atom counting. Strontium isotope shift measurements are extended into the strongly deformed region of the neutron rich isotopes up to ^{100}Sr. The radii are generally well described by the droplet model including empirical deformations obtained from B(E2) values.

Submitted to Phys. Rev. Lett.
(May 1988)

The series of strontium (Z=38) isotopes reaches from the valley of stability (at N=50) with isotopes showing spherical shape to strongly deformed isotopes within ΔN=10 on both sides of the stability line. The nuclides in this region have found considerable interest from the experimental as well as from the theoretical physics side [1-4]. The predicted strong ground state deformation at N≈40 and N≈60 [5] has been established in a series of nuclear spectroscopy experiments [6-8] which yield quadrupole deformations of $\beta \approx 0.4$ from the reduced transition probabilities. Ground state deformations in isotopic series are reflected also in the changes of mean square charge radii $\delta\langle r^2\rangle$ derived from optical isotope shift measurements [9]. A model dependent interpretation of the $\delta\langle r^2\rangle$ values has to be carried out and a first approach is commonly done in the frame of a macroscopic model, e.g. the droplet model [10]. In the Sr case, the unique situation of the availability of deformation data from B(E2) values in the regions of strong deformation as well as in the transitional region of the neutron deficient isotopes allows a stringent test of this approach, provided that the isotope shift measurements can be extended into both deformation regions far off stability. So far isotope shift data for $^{78-90}$Sr are available from experiments using optical detection [11,12].

In this letter, we report upon extended isotope shift measurements including the strongly-deformed neutron-rich isotopes up to ^{100}Sr. We introduce a new method of non-optical detection in laser-spectroscopy experiments directly on the fast-ion beams of an on-line isotope separator. The techniques using optical detection are limited by the moderate overall fluorescent photon counting efficiency and the unavoidable background from scattered laser light [13]. The basic idea behind current experimental developments is to increase the sensitivity in on-line applications by turning over to non-optical detection schemes [14-19].

Our scheme is based on detecting resonant laser optical pumping by state-selective neutralization and particle counting. This technique is dedicated to measurements on alkaline-earth ions [19], and it is complementary to the recently developed collisional ionization technique for rare gases [18].

The experiments are performed at the ISOLDE on-line isotope separator [20] at CERN. Using the 600 MeV proton beam of the CERN synchro-cyclotron, neutron-rich strontium isotopes are produced by fission reactions in a hot uranium carbide target, whereas the neutron deficient isotopes are produced by spallation reactions in a niobium-powder target. Fast ion beams, produced by a surface ionization source, 60 keV acceleration and mass separation, are deflected to interact collinearly with the light from a cw dye laser, as shown schematically in fig. 1. The experimental setup allows both classical optical detection as well as particle detection of the resonant laser-ion interaction. Isotope shifts were investigated in the $5s\ ^2S_{1/2}$-$5p\ ^2P_{1/2,3/2}$ (λ = 421.7 nm and 407.9 nm) transitions of SrII. Classical collinear laser spectroscopy [21] with fluorescent photon detection could be perfomed for the isotopes ^{78}Sr up to ^{98}Sr. A search on the mass A = 100 beam gave no indication of an optical resonance signal. However the signal of ^{100}Sr was readily observed using the state selective particle detection scheme (see fig. 2).

The basic mechanisms of this experimental scheme are the following: At resonance, multiple laser excitation in the optical pumping zone is followed by deexcitation through $5p\ ^2P_J$ - $4d\ ^2D_{J'}$ and leads to strong population of the low-lying metastable states. This change in the ionic states is efficiently translated into a change in charge state of the beam particles by passage through a Na-vapour charge

exchange cell. The neutralization reaction is strongly state-selective through the dependence of the neutralization cross-sections on the energy defects for the states involved: $\sigma(4d)/\sigma(5s) \approx 1.5$ [19]. The analysis of the charge state of the beam is performed by electrostatic separation of ions and atoms which are counted via the secondary electrons emitted by impact of the particles on an aluminium tape. The isotope shift of ^{100}Sr relative to the lighter isotopes are measured by alternately using particle detection (for A = 100) and optical detection (for two reference isotopes). To have a consistency check with the purely optical detection measurements, the isotope shift of ^{98}Sr was also measured by particle detection.

Before turning over to the interpretation of the present results, we briefly discuss the sensitivity of the new method. The strong resonance signal observed for about 10^4 ions/s of ^{100}Sr is due to the fact that an appreciable fraction of about 10^{-1} of the ions effectively contributes to the resonance signal. Using isotopically pure strontium beams [22] the signal-to-background ratio (S/B) equals 0.4, requiring about 10^2 ions/s for an experiment under ideal conditions. Under the present conditions isobaric contaminants and incomplete optical pumping reduced the S/B by a factor of 10. Still this corresponds to a required yield of 5×10^2 ions/s. This has to be compared with an optical detection limit of about 10^5 ions/s due to an overall optical detection efficiency of 10^{-3} and the high background from laser straylight. The state-selective particle detection method furthermore offers a supplementary advantage with respect to future experiments on odd isotopes. Measurements on hyperfine-splitted states are often hampered by hyperfine pumping reducing the optically detected resonance signal. A two-step ground-state depopulation pumping process cancels the hyperfine pumping

and brings the resonance signal intensity of all hyperfine components to the level of the strongest line[19].

The isotope shift results for all the investigated even isotopes are presented in table 1. Changes in mean square charge radii were deduced. Contrary to the earlier results on the Sr isotopes with $N < 50$, they were obtained in the SrII transition $5s\ ^2S_{1/2} - 5p\ ^2P_{3/2}$ which is considered most reliable for the semi-empirical calculation[23] of the electronic factor F. Therefore, we have abandoned the previous analysis based on extensive studies of the SrI spectrum in combination with muonic X-ray data[24] and directly calculated $F = -1582(49)$ MHz/fm^2 following the standard procedure and using the latest tabulated values of C_{unif}[25]. In addition to the normal mass shift (NMS), a specific mass shift of SMS = -0.13(11) NMS was deduced from a King plot of our data with muonic isotope shifts[26]. Our $\delta\langle r^2\rangle$ values largely agree with those of refs. 11, 12 for the neutron-deficient isotopes (see table 1). For the neutron-rich isotopes, also the symmetry with respect to N=50 in the following droplet-model description infers a proper choice of the calibration factor F. For the isotopes listed in table 1 the changes of $\langle r^2\rangle$ relative to ^{88}Sr are shown in fig. 3. A decrease is observed when the neutron shell closure at N=50 is approached from the neutron deficient side. For higher N, $\langle r^2\rangle$ increases almost linearly except for the dramatic increase between N=58 and N=60 which corresponds to 2.7 times the average variation found in the preceeding and following neutron rich isotopes.

The variation of the $\langle r^2\rangle$ can be interpreted in the frame of the droplet model[10] by (i): a change of the volume of the charge distribution, (ii): a change of its deformation and (iii): a change in the central part of the charge distribution due to Coulomb repulsion.

Restricting the deformation part in first order to a change in quadrupole deformation and assuming a constant diffuseness parameter, $\delta\langle r^2\rangle$ can be written as:

$$\delta\langle r^2\rangle^{(88,A)} = \frac{3}{5} R_Z^{2(A)}\left(1+\frac{5}{4\pi}\langle\beta^2\rangle^{(A)}\right)+\langle r^2\rangle_{red}^{(A)} - \frac{3}{5} R_Z^{2(88)}\left(1+\frac{5}{4\pi}\langle\beta^2\rangle^{(88)}\right)-\langle r^2\rangle_{red}^{(88)} \qquad (1)$$

with R_Z the proton sharp radius, $\langle\beta^2\rangle$ the mean square quadrupole deformation parameter and $\langle r^2\rangle_{red}$ the redistribution term attributed to the respective isotopes. The droplet values for the changes in $\langle r^2\rangle$ were calculated using the model parameters given in ref. 27 and are included in fig. 3 by showing a set of isodeformation lines. From a comparison of these lines with the experimental data it is evident that the observed trend of the radii expresses mainly the change of deformation of the nuclear charge distribution. As expected from nuclear spectroscopy data, high ground state deformations of $\langle\beta^2\rangle^{1/2} \approx 0.4$ are indicated at the extrema of the isotopic chain at $A \approx 78$ and $A \approx 100$. It is also consistent with spectroscopy information that the onset of deformation seems to occur more gradually for the light isotopes, whereas a sudden change from near spherical to strongly deformed shape is observed for the neutron-rich isotopes between A=96 and A=98.
More quantitatively, the experimental $\delta\langle r^2\rangle$ values can be compared to calculated ones obtained from the droplet model using $\langle\beta^2\rangle$ from experimental B(E2) values [28,29]. To be consistent with the droplet model description of the radii, we used values calculated in the frame of this model [10,27], which are only slightly different from the tabulated ones [28]. For those isotopes for which no B(E2) values are available ($90 \leq A \leq 96$), the quadrupole deformation is estimated from the energy of the first excited 2^+ level [30]. The calculated curves are

included in fig. 3. Comparing the experimental $\delta\langle r^2\rangle$ values with the calculated ones, we state good agreement between both sets for neutron rich isotopes [31] and also for the strongest deformed isotopes on the neutron deficient side. Some disagreement is observed only in the transitional region $82 \leq A < 88$.

Apart from details the general trends of our present $\delta\langle r^2\rangle$ curve for the Sr isotopes agree rather well with those in the neighbouring odd-Z element Rb [14]. This latter has served as a test case for investigating the influence of collective zero-point motion on the development of the mean square charge radii [32]. It was concluded by Myers and Rozmej that theoretical values for the collective width $\langle\varepsilon^2\rangle$ or $\langle\beta^2\rangle$ fail to explain the sharp change in the slope of the $\delta\langle r^2\rangle$ curve at N = 50. Reasons for this discrepancy were sought in higher-order multipole contributions or in single-particle core polarization effects. For the doubly-even Sr isotopes the measured B(E2) values offer empirical information about the E2 strength connected with the nuclear ground state [33]. It is obvious from fig. 3 that the droplet model with these empirical values for $\langle\beta^2\rangle$ gives a substantially better agreement with the experimental data. Therefore, it should be examined to what extent the collective zero-point motion based on a Nilsson single-particle potential reproduces the experimentally observed E2 strength.

Possible reasons for the remaining mismatch in the transitional region $82 \leq A < 88$ where already discussed for the stable Sr isotopes in ref. 34 and attributed to changes in the diffuseness of the charge distribution. In how far this picture can be extended to the isotopes further off stability will be investigated in a more comprehensive analysis of the experimental data which includes also hfs data now

being evaluated [35]. In this respect we expect also a better understanding of the variation of the $\langle r^2 \rangle$ in Sr from a combined interpretation of the data in the droplet as well as in a microscopic model.

This work was supported by the Belgian Interuniversity Institute for Nuclear Science (IIKW), the Canadian Natural Sciences and Engineering Research Council (NSERC), and the German Federal Minister for Research and Technology (BMFT) under the contract number 06MZ458I. One of us (R.E.S.) is a research associate of the Belgian Foundation for Scientific Research (NFWO).

References.

[1] K. Heyde, J. Moreau and M. Waroquier, Phys. Rev. C29, 1859 (1984)

[2] W. Nazarevitch et al., Nucl. Phys. A435, 397 (1985)

[3] K.P. Lieb, L. Lühmann and B. Wörmann, in Nuclei Off the Line of Stability, Chicago, 1985, eds. R.A. Meyer and D.S. Brenner (American Chemical Society, Washington D.C., 1986) 233

[4] P. Bonche et al., Nucl. Phys. A443, 39 (1985)

[5] P. Möller and J.R. Nix, At. Data Nucl. Data Tables 26, 165 (1981)

[6] C.J. Lister et al., Phys. Rev. Lett. 49, 308 (1982)

[7] F. Schussler et al., Nucl. Phys. A339, 415 (1980)

[8] R.E. Azuma et al., Phys. Lett. 86B, 5 (1979)

[9] R. Neugart, in Lasers in Nuclear Physics, eds. C.E. Bemis jr. and H.K. Carter, (Harwood, Chur, 1982) 231

[10] W.D. Myers and K.H. Schmidt, Nucl. Phys. A410, 61 (1983)

[11] M. Anselment et al., Z. Phys. A326, 493 (1987)

[12] D.A. Eastham et al., Phys. Rev. C36, 1583 (1987)

[13] Fluorescent Atom Coincidence Spectroscopy, a method to suppress the background, was demonstrated in ref. 12

[14] C. Thibault et al., Phys. Rev. C23, 2720 (1981)

[15] V.I. Balykin et al., Sov. Phys. Usp. 23, 651 (1980)

[16] E. Arnold et al., Phys. Lett. B197, 311 (1987)

[17] K. Wallmeroth et al., Phys. Rev. Lett. 58, 1516 (1987)

[18] R. Neugart, W. Klempt and K. Wendt, Nucl. Instr. Meth. B17, 354 (1986)

[19] R.E. Silverans, P. Lievens and L. Vermeeren, Nucl. Instr. Meth. B26, 591 (1987)

[20] H.L. Ravn, Phys. Rep. 54, 201 (1979)

[21] A.C. Mueller et al., Nucl. Phys. A403, 234 (1983)

[22] S.V. Andreev, V.I. Mishin and V.S. Letokhov, Opt. Comm. 57, 317 (1986)

[23] K. Heilig and A. Steudel, At. Data Nucl. Data Tables 14, 613 (1974)

[24] D. Bender et al., Z. Phys. 318, 291 (1984)

[25] S.A. Blundell et al., Z. Phys. A321, 31 (1985)

[26] R. Engfer et al., At. Data Nucl. Data Tables 14, 509 (1974)

[27] D. Berdichevsky and F. Tondeur, Z. Phys. A322, 141 (1985)

[28] S. Raman, At. Data Nucl. Data Tables 36, 1 (1987) and refs. therein

[29] H. Ohm et al., Z. Phys. A327, 483 (1987)

[30] L. Grodzins, Phys. Lett. 2, 88 (1962)

[31] The decrease in deformation from ^{98}Sr to ^{100}Sr recently reported in ref. 29 is not confirmed by our results.

[32] W.D. Myers and P. Rozmej, Nucl. Phys. A470, 107 (1987)

[33] K. Kumar, Phys. Rev. Lett. 28, 249 (1972)

[34] F. Buchinger et al., Phys. Rev. C32, 2058 (1985)

[35] Spin assignments have been reported in Z. Phys. A327, 361 (1987)

Table 1. Isotope shifts and changes in mean square charge radii relative to A=88 for the even strontium isotopes.

Mass number	Isotope shift (MHz)	$\langle r^2\rangle^A - \langle r^2\rangle^{88}$ (fm^2) This work [b]	Ref. 11 [c]	Ref. 12 [d]
78	-893(12)	0.242(8)[41]		0.237(9)
80	-782(11)	0.243(7)[33]	0.227(20)	0.249(6)
82	-574(10)	0.179(6)[24]	0.169(13)	0.182(6)
84	-373(5)	0.116(3)[16]	0.110(9)	0.116(4)
86	-171(3)	0.050(2)[8]	0.047(5)	0.046(6)
90	-349(6)	0.277(4)[12]	0.23(9)	
92	-636(8)	0.512(5)[21]		
94	-876(9)	0.715(6)[30]		
96	-1198(10)	0.968(6)[40]		
98	-2155(13) -2166(11) [a]	1.625(6)[59]		
100	-2415(23) [a]	1.832(15)[69]		

a) Measured with the particle detection method.

b) Experimental errors using the procedure of ref. 21 are given between round brackets; errors including systematic errors due to uncertainties in the evaluation of $\delta\langle r^2\rangle$ from the I.S. are given between square brackets.

c) Data of set 1, King-plot errors included. Data of set 2 are ~30% higher.

d) Experimental errors only.

Figure captions.

Fig. 1. Schematic experimental set-up.

Fig. 2. Particle detection $^2S_{1/2}$ - $^2P_{3/2}$ resonance signal of ^{100}SrII (2s/channel laser frequency scan).

Fig. 3. Experimental changes in mean square charge radii (Error bars include systematic errors). Droplet model isodeformation curves (broken lines) and a comparison with $\delta\langle r^2\rangle$ calculated from B(E2) values (error band indicated as full lines) are added. $\langle\beta^2\rangle^{1/2} = 0.128(4)$ for ^{88}Sr was used as reference.

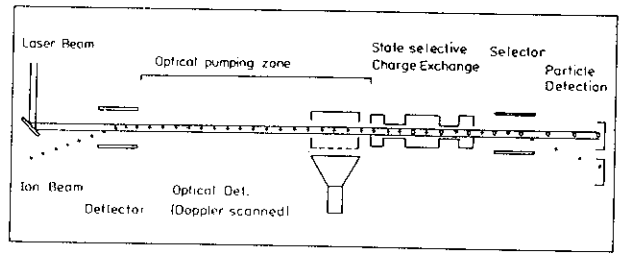

Fig. 1.

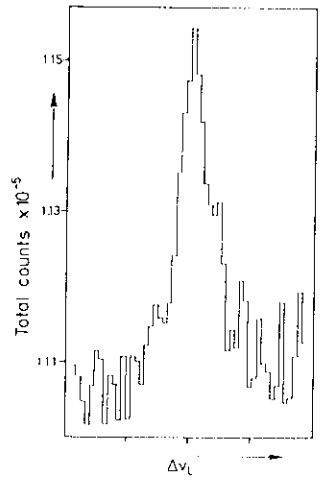

Fig. 2.

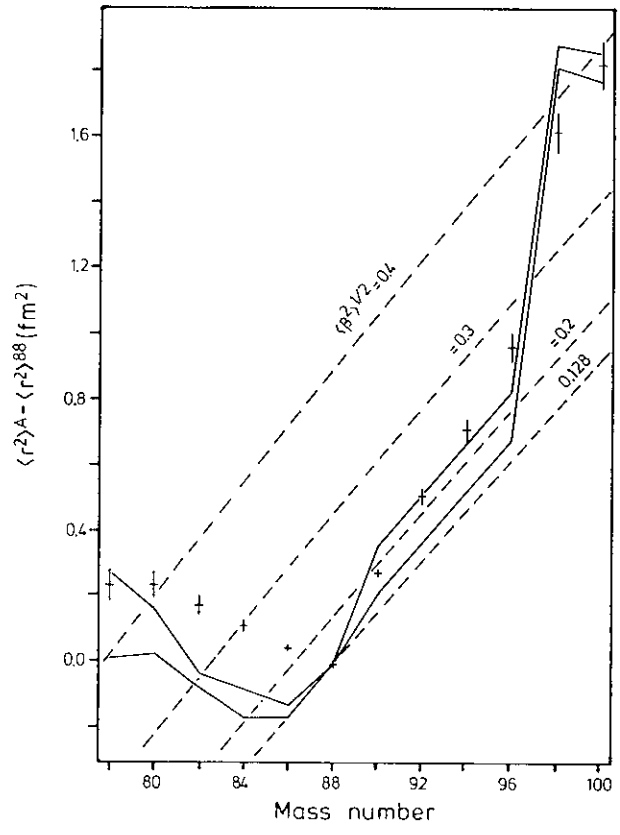

Fig. 3.